



ELSEVIER

Available online at [www.sciencedirect.com](http://www.sciencedirect.com)

SCIENCE @ DIRECT®

Nuclear Instruments and Methods in Physics Research B 229 (2005) 219–226

**NIM B**  
Beam Interactions  
with Materials & Atoms

[www.elsevier.com/locate/nimb](http://www.elsevier.com/locate/nimb)

# Coherent production of relativistic positronium atoms by photons and electrons in a crystal

Yu.P. Kunashenko <sup>a,b</sup>

<sup>a</sup> Nuclear Physics Institute, Tomsk Polytechnic University, Lenin Ave., 2 a P.O. Box 25, Tomsk 634050, Russia

<sup>b</sup> Tomsk Polytechnic University Lenin Ave., 30, Tomsk 634050, Russia

Received 22 January 2004; received in revised form 11 November 2004

Available online 12 January 2005

## Abstract

Theory of coherent type B positronium atom production by high energy photon and relativistic electron in a real (three dimensional) crystal has been developed. On the base of developed theory the orientation dependence of cross-section is studied. It is shown, that small change of the photon energy in the vicinity of coherent peak results in change of character of the coherent type B Ps photoproduction orientation dependence.

© 2004 Elsevier B.V. All rights reserved.

PACS: 12.20.-m; 61.80.Fe

Keywords: Relativistic positronium atom; High energy photon; Relativistic electron; Coherent effect

## 1. Introduction

Many physical processes, accompanying passage of the high energy particle through an alignment crystal with small angle with respect to crystal axis or plane, change in comparison with ones in an amorphous target. In fact, in this case coherent effects occur (see for example [1,3,2]). The coherent effect manifests itself in development of coherent maximums in the dependence of the process cross-section under consideration at the

definite particle energies or incident angles. The reason of existence of the coherent effect in a crystal is connected with quantization of the momentum transferred to crystal, and coherent maximum arises, when momentum transferred coincidences with one of the reciprocal lattice vector.

Now coherent effects are divided into two types: A and B [4]. Coherent type A effect appears in the case, when incident particle has small angle with respect to a crystal plane and large one with respect to crystal axis. For coherent type A main contribution into cross-section comes from reciprocal lattice vectors, which are in the plane

E-mail address: [kun@npi.tpu.ru](mailto:kun@npi.tpu.ru)

perpendicular to a particle trajectory. That means that quantization of the momentum transferred takes place in this plane. If incident particle enters into crystal at small angle with respect to crystal axis, then coherent type B effect appears. In a last case quantization of the momentum transferred occurs along crystal axis. It should be notice that, ordinary coherent type B effect takes place at sufficiently low energies of the initial (final) particles, than coherent type A effect.

For the first time the possibility of positronium atom (Ps) creation by a photon in a field of atom was considered in [5]. Theory of relativistic singlet Ps production was developed by Olsen [6] and Lubosshits [7] in the first Born approximation (in this approximation only singlet Ps can be produced). The cross-section of the singlet and triplet Ps creation by relativistic electron in the Coulomb field was calculated by Holvik and Olsen [8]. More exact theory of the singlet and triplet Ps production in a field of atom by photons and electrons is developed by Kuraev and co-authors [9–11] and independently by Olsen [12,13].

The possibility of coherent type B creation of Ps in a crystal first was predicted in [14] for photoproduction and in [15] for production by relativistic electrons. In the papers [14,15] it was shown that the sharp coherent peaks appear at definite Ps energies and emission angles. More detailed theoretical investigations of the Ps coherent type B photoproduction and production by relativistic electrons in the crystals have been performed in [16,17].

In [14–17] the one string approximation was used, which takes into account an interaction of incident photon (electron) with a single crystal axis (1D-model). The 1D-model is valid, when an initial angle  $\Theta_0$  of incident photon or electron with respect to a crystal axis is small ( $\vartheta_0 \ll d/l$ , here  $d$  is a distance between crystal axis and  $l$  is a length of the crystal). In fact, for the such small incident angle photon interacts only with separate crystal axis and one can neglect its interaction with other crystal axes. But for the greater incident angles ( $\vartheta_0 \geq d/l$ ) it is necessary to take into account the interaction of the photon with all crystal axes and, therefore, 3D-model should be used.

In a present paper (in a first Born approximation) the detailed theory of coherent type B Ps production by photon and high energy electron in a real (three dimensional) crystal was considered. We call this approach 3D-model.

The advantages of the 3D-model in comparison with the 1D-model are as follows: the 3D-model allows more correct calculation of the energy and angular distributions of created Ps, and also to study orientation dependence of the cross-section of coherent type B photoproduction and production by relativistic electron of Ps in a crystal (the dependence of cross-section on the angle of photon or electron momentum with respect to a crystal axis and planes).

## 2. Theory

The differential over emission angles cross-section of the Ps production by a photon with an energy  $\omega$  in the Coulomb field of an atom is [6,7]

$$\frac{d\sigma_1}{d\Omega} = \frac{Z^2 \alpha^6 \beta^3}{8m^2 \gamma^4} \frac{\sin^2 \Theta}{(1 + \beta^2 - 2\beta \cos \Theta)^2 (1 - \beta \cos \Theta)^2}. \quad (1)$$

Here,  $\alpha$  is the fine structure constant,  $\gamma$  and  $\beta$  are the relativistic factor and velocity of created Ps,  $\Theta$  is Ps emission angle with respect to a photon momentum,  $m$  is an electron rest mass,  $Z$  is nuclear charge of the target atom (the units  $\hbar = c = 1$  are used). The transferred to an atom momentum squared is

$$q^2 = (E^2 + p^2 - 2Ep \cos \Theta) = E^2(1 + \beta^2 - 2\beta \cos \Theta), \quad (2)$$

here,  $E = \omega$  is the Ps energy. If the  $z$ -axis is parallel to a photon momentum,  $\vec{k} \parallel OZ$ , then the components of the momentum transferred are

$$\vec{q} = \begin{cases} q_x = -p \sin \Theta \cos \varphi; \\ q_y = -p \sin \Theta \sin \varphi; \\ q_z = \omega - p \cos \Theta = E(1 - \beta \cos \Theta). \end{cases} \quad (3)$$

Here,  $p$  is the momentum of created Ps,  $\varphi$  is the angle of Ps momentum in a plane perpendicular to photon momentum. For the following consider-

ation it is convenient to introduce the transverse component of the momentum transferred  $\vec{q}_\perp = \{q_x, q_y\}$ . From Eq. (3) one has  $q_\perp^2 = q_x^2 + q_y^2 = p^2 \sin^2 \Theta$ . After substitution of Eqs. (2) and (3) into Eq. (1), and taking into account the relation between  $d\Omega$  and  $\vec{q}_\perp = dq_x dq_y$ , we express the differential cross-section of Ps production by high energy photon in the Coulomb field of an atom in variables of the transferred momentum:

$$d\sigma_1 = \frac{Z^2 \alpha^6 E}{8\beta m^2 \gamma^4} \frac{q_\perp^2}{q^4 q_z^2} \frac{dq_x dq_y}{\sqrt{p^2 - q_\perp^2}}. \quad (4)$$

It is well known that in an aligned crystal a cross-section of any coherent process can be written as a sum of coherent and incoherent parts [1,4]:

$$d\sigma_{\text{cr}} = d\sigma_{\text{coh}} + d\sigma_{\text{incoh}},$$

here  $d\sigma_{\text{coh}}$  is a coherent part of the cross-section:

$$d\sigma_{\text{coh}} = I(\vec{q}) \exp(-q^2 \bar{u}^2) d\sigma_1 \quad (5)$$

and  $d\sigma_{\text{incoh}}$  is an incoherent one:

$$d\sigma_{\text{incoh}} = N \left[ 1 - \exp(-q^2 \bar{u}^2) \right] d\sigma_1. \quad (6)$$

In Eqs. (5) and (6),  $\exp(-q^2 \bar{u}^2)$  is Debye–Waller factor, which takes into account the thermal vibrations of the crystal atoms,  $\bar{u}^2$  is the mean-squared deviation of the crystal atom from the equilibrium position,  $I(\vec{q})$  is an interferential multiplier responsible for coherent effect appearance. In the 3D-model  $I(\vec{q})$  should be written in a following form ( $N_x, N_y \gg 1, N_z$  is large but fixed):

$$I(\vec{q}) = N_x N_y \frac{(2\pi)^2}{d_x d_y} \sum_{n,l} \delta(q_x - g_x n) \delta(q_y - g_y l) \times \frac{\sin^2(N_z q_z d_z / 2)}{\sin^2(q_z d_z / 2)} |S(\vec{q})|^2. \quad (7)$$

In the last equation  $N_x, N_y, N_z$  are the numbers of the crystal atoms in  $x, y, z$  directions respectively, which contribute into coherent process:  $g_x = \frac{(2\pi)}{d_x} n, g_y = \frac{(2\pi)}{d_y} l, n, l = 1, 2, 3, \dots$  are the components of the reciprocal lattice vector  $\vec{g}$  in  $x$  and  $y$  directions and  $d_x, d_y, d_z$  are the lattice constant in  $x, y, z$  directions respectively,  $S(\vec{q})$  is a crystal structure factor.

In the proposed experiment [17] it is planned to measure the Ps yield within small angular cone. To compare our results with [17] (based on 1D-model) we integrate  $d\sigma_{\text{cr}}$  over the Ps emission angles. In our case the integration over Ps emission angles is replaced by integration over the transverse transferred momentum  $\vec{q}_\perp$ . After substitution of Eq. (7) into Eq. (5) and integration over  $\vec{q}_\perp$  we arrive at

$$\begin{aligned} \sigma_{\text{coh}} &= \int_0^{2\pi} d\varphi \int_0^{\Theta_m} \sin \Theta d\Theta \frac{d\sigma_{\text{coh}}}{d\Omega} \\ &= \int_0^{q_\perp^{\text{max}}} d\vec{q}_\perp \frac{d\sigma_{\text{coh}}}{d\vec{q}_\perp} \\ &= N_x N_y \frac{(2\pi)^2}{d_x d_y} \sum_{n,l} \sigma(\vec{q}_\perp^{n,l}, q_z) |S(\vec{q}_\perp^{n,l}, q_z)|^2 \\ &\quad \times \exp\left(-\left[(\vec{q}_\perp^{n,l})^2 + q_z^2\right] \bar{u}^2\right) \frac{\sin^2(N_z q_z (\vec{q}_\perp^{n,l}) d_z / 2)}{\sin^2(q_z (\vec{q}_\perp^{n,l}) d_z / 2)}. \end{aligned} \quad (8)$$

Here,  $\vec{q}_\perp^{n,l}$  is the transverse transferred momentum with components:  $q_x = g_x n$  and  $q_y = g_y l$ ,  $\Theta_m$  is the maximal emission angle of Ps with respect to the incident photon momentum. The value of  $\Theta_m$  is determined by experimental setup. As it follows from Eq. (3):

$$q_z(\vec{q}_\perp^{n,l}) = E \left[ 1 - \beta \arccos\left(\left(\frac{\vec{q}_\perp^{n,l}}{p}\right)^{1/2}\right) \right]. \quad (9)$$

If the atomic screening is chosen in the form  $V(r) = \frac{Ze}{r} \exp(-\frac{r}{R})$ , the  $\sigma(\vec{q}_\perp^{n,l}, q_z)$  has a form

$$\sigma(\vec{q}_\perp, q_z) = \frac{Z^2 \alpha^6}{8\beta m^2 \gamma^4} E \frac{q_\perp^2}{(q^2 + R^{-2})^2 q_z^2} \frac{1}{\sqrt{p^2 - q_\perp^2}}, \quad (10)$$

here  $R$  is an atom screening radius.

The summation in Eq. (8) should be performed taking into account the condition

$$q_x^2 + q_y^2 = q_\perp^2 \leq E^2 \beta^2 \sin^2 \Theta_m.$$

The incoherent part of the Ps photoproduction cross-section in a crystal has a form

$$\sigma_{\text{incoh}} = \int_0^{2\pi} d\varphi \int_0^{\Theta_m} \sin \Theta d\Theta \frac{d\sigma_{\text{incoh}}}{d\Omega}. \quad (11)$$

Eqs. (8) and (11) describe the coherent Ps production by a photon in a crystal. Further calculations based on Eqs. (8) and (11) are carried out numerically.

### 3. Numerical results

#### 3.1. Ps coherent production by a photon

In order to demonstrate the coherent effect let us introduce the ratio  $R$  of the Ps coherent type B production cross-section by high energy photon in a crystal to one in an amorphous target of equivalent thickness, which contains the same number  $N$  of atoms as a crystal

$$R = \frac{\sigma_{\text{cr}}}{N\sigma_1} = \frac{\sigma_{\text{coh}} + \sigma_{\text{incoh}}}{N\sigma_1}.$$

In Fig. 1(a) it is shown the dependence of the ratio  $R$  on the photon energy calculated for Si crystal, oriented by  $\langle 100 \rangle$  axis with respect to a photon momentum. The maximal emission angle of Ps is  $\Theta_m = 5$  mrad. The number of atoms in a crystal axis is  $N_z = 100$ . As it follows from Eq. (8) the cross-section has sharp maximum when  $q_z(\vec{q}_\perp^{m,l})d_z/2 = \pi m/2$ ,  $m = 1, 2, 3, \dots$ . Using (9), one have

$$E(1 - \beta \arccos \Theta) \frac{d_z}{2} = \frac{\pi}{2} m, \quad m = 1, 2, 3, \dots;$$

here  $\Theta = \arccos(\vec{q}_\perp^{n,l}/p)^{1/2}$  is Ps emission angle with respect to crystal axis. The Ps emission angle with respect to photon momentum is very small, therefore in the case when photon momentum is parallel to crystal axis in first approximation one can consider  $\Theta = 0$ . Then

$$q_z \approx E(1 - \beta) \frac{d_z}{2} \approx \frac{E}{4\gamma^2}.$$

Now the condition of appearance of coherent peak coincides with one which follows from 1D-model [14–17]:

$$\omega_m = \frac{4m^2 + g_m^2}{2g_m}, \quad k = 1, 2, 3, \dots; \quad (12)$$

here  $g_m = \frac{(2\pi)}{d_y} m$  is component reciprocal vector parallel to crystal axis.

The enhancement due to coherent effect of Ps yield in a crystal is very large and, in our case,  $R \simeq 20$  in a vicinity of the first coherent peak near  $E = 229$  MeV.

The detailed structure of the coherent peak in the vicinity of the first coherent maximum near the photon energy  $\omega \approx 229$  MeV it is shown in

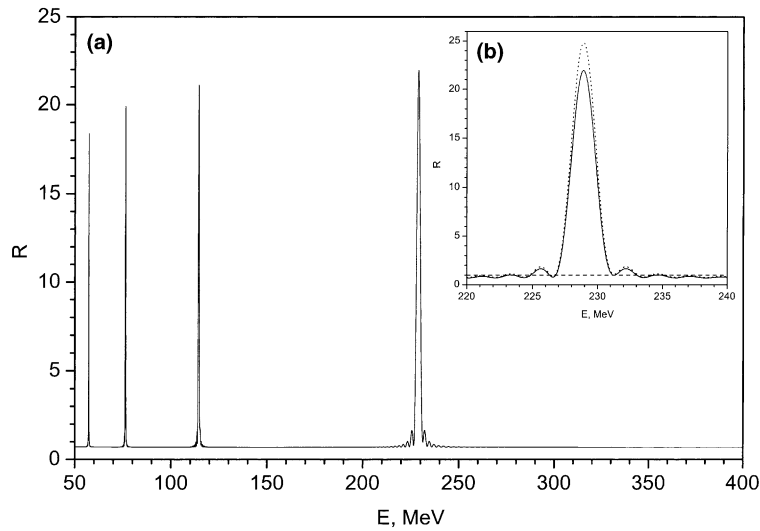


Fig. 1. (a) The dependence of the ratio  $R$  of the cross-section of type B coherent photoproduction to one in amorphous target of equivalent thickness as a function of the photon energy. The crystal Si(100), maximal emission angle of Ps is  $\Theta_m = 5$  mrad,  $N_z = 100$ , crystal temperature is  $T = 0$  K. (b) The detailed structure of the first coherent peak in the vicinity of the coherent maximum near the photon energy  $\omega \approx 229$  MeV: solid line—result of 3D-model, dotted line—result of 1D calculations. Dashed line shows the level  $R = 1$ .

Fig. 1(b) solid line. In order to compare the result of 3D-model and 1D-model in Fig. 1(b) the ratio  $R$  calculated in framework of 1D-model is shown by dotted line. The dashed line shows the level  $R = 1$ . As it follows from Fig. 1(b) the calculated values of  $R$  according to 1D and 3D-models are in a good agreement. Fig. 1(b) shows that as in 1D-model in a 3D-model there is a fine structure in a dependence of the cross-section of the cross-section of coherent type B photoproduction of Ps on incident photon energy. The reason of appearance of fine structure of the cross-section is as follows: the sum in Eq. (8) contains the multiplier  $\frac{\sin^2(N_z q_z(\vec{q}_\perp^{\perp,l})d_z/2)}{\sin^2(q_z(\vec{q}_\perp^{\perp,l})d_z/2)}$  which has subsidiary ones, when  $N_z q_z(\vec{q}_\perp^{\perp,l})d_z/2 = \pi/2 + \pi n$ ,  $n = 1, 2, 3 \dots$  in addition to sharp maximums (8).

Fig. 2 presents the orientation dependence of the cross-section of coherent type B photoproduction of Ps integrated over Ps emission angles. In our calculation, the maximal emission angle of Ps is  $\Theta_m = 5$  mrad. The parameters of the crystal are as in Fig. 1; different curves correspond to different photon energies in the vicinity of the first coherent peak. Fig. 2 shows that a small change of the photon energy in the vicinity of coherent peak results in change of a character of the orientation dependence of coherent type B Ps photoproduction. For example, for the photon energies 227 MeV and 231 MeV there is a minimum at  $\vartheta \rightarrow 0$  with respect to the crystal axis, while for photon energies 228, 229 and 230 MeV we have a maximum at angle  $\vartheta \rightarrow 0$ .

The reason of such orientation dependence character is as follows. When a photon energy approaches to the energy of coherent maximum  $\omega_k$  (from the side of a smaller energies), the cross-section value slowly decreases. But when energy reaches  $\omega_k$  the coherent maximum occurs and the cross-section greatly increases. Further increasing of the photon energy results in decreasing of the cross-section. On the other hand, with small increasing the incident photon angle with respect to crystal axis, the momentum projection onto crystal axis changes as  $k_{\parallel} = k \cos(\vartheta)$ , here  $k = |\vec{k}| = \omega$ . In the first approximation we suppose that 1D-model is still correct. Therefore, increasing the incident angle  $\vartheta$  is equivalent to small decreasing of

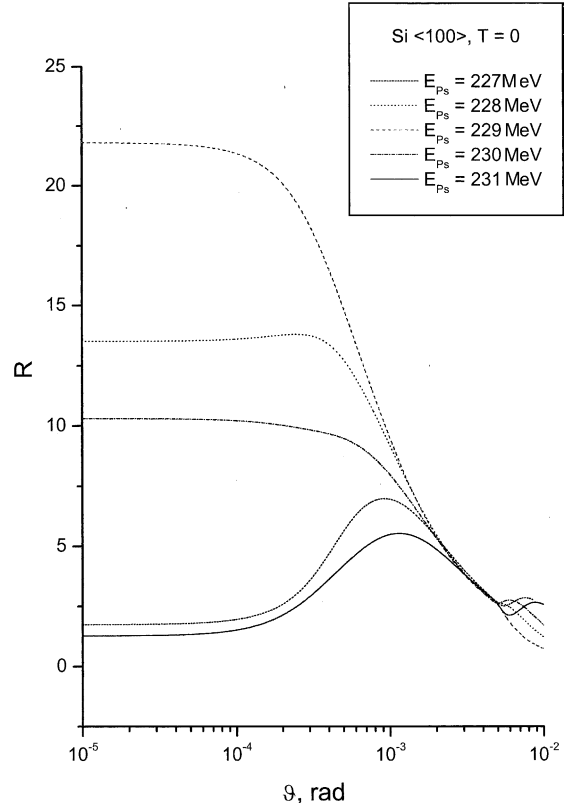


Fig. 2. Orientation dependence of the ratio  $R$  of the cross-section of type B coherent Ps photoproduction in a crystal to one in an amorphous target of equivalent thickness. The parameters of the crystal are the same as in Fig. 1. Shot dashed line corresponds to created Ps energy  $E = 227$  MeV, dotted line  $E = 228$  MeV, dashed line  $E = 229$  MeV, dashed-dotted line  $E = 230$  MeV and solid line  $E = 231$  MeV, respectively.

the photon energy. As a result, we obtain the orientational dependence near  $\vartheta = 0$  as shown in Fig. 2. The cross-section at  $\vartheta = 0$  has maximum for the photon energy very close to the energy of the coherent maximum and minimal if the photon energy differs from  $\omega_n$ . When angle  $\vartheta$  sufficiently increase ( $\vartheta \gg \vartheta_0$ ) 3D-model should be used and picture becomes more complicated.

### 3.2. Ps production by relativistic electron

The triplet and singlet Ps can be produced by relativistic electron passing through a crystal [15]. We restrict our consideration only by singlet Ps

coherent production. In this case one can derive the cross-section in a framework of the virtual photon method [8,15]:

$$\frac{d\sigma_E^{\text{cr}}}{dE_1} = \sigma_{\text{cr}}(\omega)n(\omega), \quad (13)$$

here  $n(\omega)$  is the virtual photon spectrum associated with incident relativistic electron

$$n(\omega)dE_1 = \frac{\alpha}{2\pi} \frac{dE_1}{E_1} \times \left\{ \left[ 1 + \left( \frac{E_1 - \omega}{\omega} \right)^2 \right] \ln \frac{E_1(E_1 - \omega)}{\omega^2} - 2 \left( \frac{E_1 - \omega}{\omega} \right) \right\}, \quad (14)$$

here  $E_1$  is an initial electron energy,  $\omega$  is a virtual photon energy. The cross-section  $\sigma_{\text{cr}}(\omega)$  has been studied in Section 2. Therefore further investigation is straight-forward.

The cross-section of coherent of type B production of Ps by relativistic electrons as a function of created Ps energy is shown in Fig. 3. The energy of the incident electron is  $E_1 = 1$  GeV (Fig. 3(a)) and is  $E_1 = 10$  GeV (Fig. 3(b)). The cross-section is integrated over emission angles of Ps and the maximal emission angle of Ps is  $\Theta_m = 5$  mrad. Target is Si $\langle 100 \rangle$ . The number of atoms in a crystal axis  $N_z = 100$ . Again, as in a case of photoproduction, one can see sharp coherent peaks at the definite energies of created Ps.

Dashed lines show a cross-section of the Ps production by electrons in an amorphous target of equivalent thickness, which contains the same number  $N$  of atoms as a crystal axis:

$$\frac{d\sigma_E}{dE_1} = N\sigma_1(\omega)n(\omega).$$

As it follows from Fig. 3, with increasing of the electron energy the position of coherent peak remains the same, while the value of the cross-section increases. In fact, the number of virtual photons is increased with increasing the energy of electrons (see Eq. (14)) and consequently the Ps production cross-section by electron in a crystal increases too. The positions of coherent peaks do not depend on the electron energy and are determined by crystal parameters (lattice constant). Indeed,  $n(\omega)$  is a smooth function of the virtual photon energy and depends only from the incident

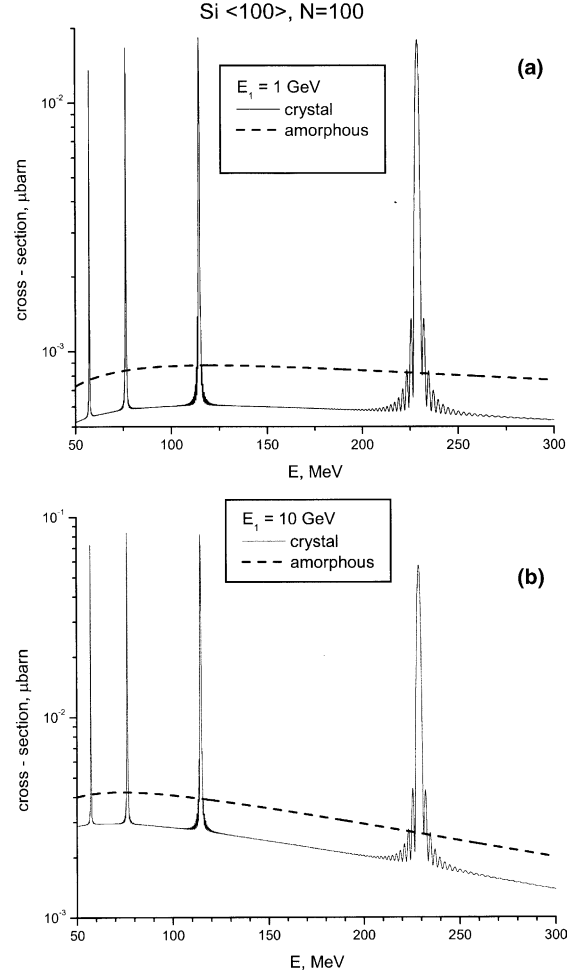


Fig. 3. The cross-section of coherent type B production of Ps by relativistic electrons as a function of created Ps energy for two electron energies  $E_1 = 1$  GeV (Fig. 4(a)) and  $E_1 = 10$  GeV (Fig. 4(b)). Dashed lines show the cross-section of the Ps production by electrons in an amorphous target of equivalent thickness, which contains the same number  $N$  of atoms as a crystal. The maximal emission angle of Ps is  $\Theta_m = 5$  mrad. The parameters of the crystal are the same as in Fig. 1.

electron energy, therefore all coherent effects are determined by the Ps production cross-section by (virtual) photon. According to Section 3.1 this cross-section has sharp coherent maxima at definite photon energy  $\omega_k$ . The values of  $\omega_k$  are depends only from crystal parameters.

In order to compare the coherent type B Ps production by photons and electrons ( $E_1 = 1$  GeV),

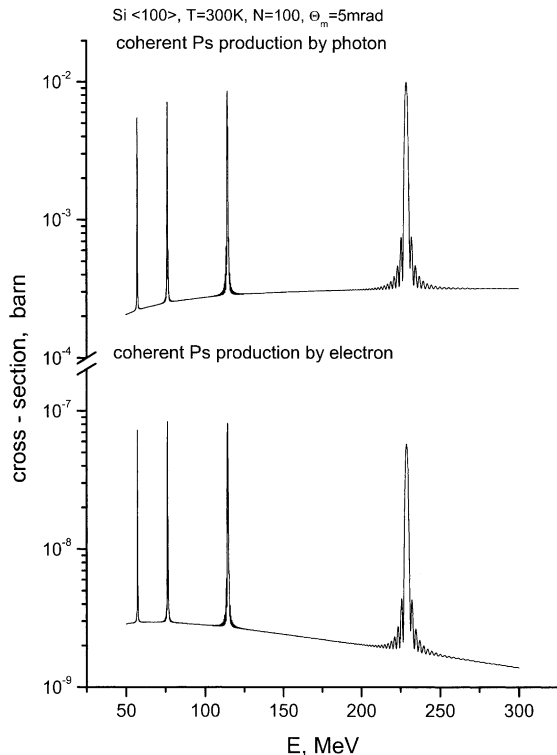


Fig. 4. The cross-sections of coherent Ps photoproduction (upper curve) and of coherent Ps production by relativistic electron (lower curve) as a function of created Ps energy. Energy of electron is  $E_1 = 1$  GeV. Other parameters are the same as in Fig. 1.

we show in Fig. 4 the cross-sections of coherent Ps photoproduction (upper curve) and of coherent Ps production by relativistic electron (lower curve) in dependence of created Ps energy. The positions of coherent peaks for the coherent photoproductions and electroproduction coincide, while the shapes of cross-sections are little bit different due to the own shape of the virtual photon spectrum associated with incident relativistic electron.

#### 4. Conclusions

Our results based on 3D-model calculations confirm the prediction of 1D-model [14,16,17] on existence of sharp peaks at definite energies of cre-

ated Ps and emission angles for the coherent type B production of Ps by high energy photon or electron. The results of calculations according 1D and 3D-models of Ps energy spectra are in a good agreement.

Important advantage of 3D-model in comparison to 1D-model is, that 3D-model allows to calculate the orientation dependence of the cross-section of coherent photoproduction and production of Ps by relativistic electrons in a crystal for the rather large incident angles. Numerical results show that a small change of a photon energy in the vicinity of coherent peak results in change of the orientation dependence of the coherent type B photoproduction of Ps.

In the case of coherent type Ps production by relativistic electrons, as in a case of photoproduction, sharp coherent peaks appear at the definite energies of created Ps. The positions of coherent peaks do not depend on the electron energy. With increase of the electron energy the value of cross-section increases.

The obtained formulas can be used also for the study of coherent type A process, which takes place when initial particle has small incident angle with respect to the crystal plane. In this case a coherent effect appears at sufficiently more high energy. The investigation of the coherent type A photoproduction of Ps and a type A production of Ps by relativistic electron will be done in a separate paper.

The brilliant coherent effect was predicted for coherent type B  $e^+e^-$  pair by high energy in a crystal under condition of strong collimation of created electron and positron [16,17]. This effect was recently confirmed in the experiment [18]. The coherent Ps production by photon or electron one can consider as a limiting case of extremely hard collimation of created  $e^+e^-$  pair.

#### Acknowledgements

The author is grateful to Prof. Yu. L. Pivovarov for the fruitful discussions. The work is supported by the grant from RFBR, contract no. 01-02-17562.

## References

- [1] L.M. Ter-Mikelian, High Energy Electromagnetic processes in Condensed Media, Wiley Interscience, New York, 1972.
- [2] V.N. Baier, V.M. Katkov, V.M. Strakhovenko, Electromagnetic Processes at High Energy in Oriented Single Crystals, World Scientific, Singapore, 1998.
- [3] H. Uberall, Phys. Rev. 103 (1956) 1055.
- [4] A.W. Saenz, H. Uberall, Theory of coherent bremsstrahlung, in: A.W. Saenz, H. Uberall (Eds.), Coherent Radiation Sources, Springer-Verlag, Berlin, 1985, p. 5.
- [5] G.V. Meledin, V.G. Serbo, A.K. Slivkov, Pis'ma Zh. Eksp. Teor. Fiz. 13 (1971) 98; JEPT Lett. 13 (1971) 68.
- [6] H.A. Olsen, Phys. Rev. D 33 (1986) 2033.
- [7] V.L. Lyuboshits, Yad. Fiz. 45 (1987) 682.
- [8] E. Holvik, H.A. Olsen, Phys. Rev. D 35 (1987) 2124.
- [9] S. Gevorkyan, E. Kuraev, A. Tarasov, A. Shilleer, V.G. Serboet, in: M.A. Ivanov, E.A. Kuraev (Eds.), Workshop Hadronic atoms and positronium in the standard model, E2-98-254, Dubna, 1998, p. 183.
- [10] S. Gevorkyan, E. Kuraev, A. Schiller, V.G. Serbo, A. Tarasov, Phys. Rev. A 58 (1998) 1556.
- [11] G.L. Kotkin, E.A. Kuraev, A. Schiller, V.G. Serbo, A. Tarasov, Phys. Rev. C 59 (1999) 2734.
- [12] H.A. Olsen, Phys. Rev. A 63 (2001) 032101.
- [13] H.A. Olsen, Phys. Rev. A 60 (1999) 1883.
- [14] Yu.P. Kunashenko, Yu.L. Pivovarov, Yad. Fiz. 51 (1990) 627.
- [15] G.I. Sandnes, H.A. Olsen, Phys. Rev. A 48 (1993) 3725.
- [16] Yu.P. Kunashenko, Yu.L. Pivovarov, Nucl. Instr. and Meth. B 114 (1996) 237.
- [17] Yu.L. Pivovarov, Yu.P. Kunashenko, I. Endo, T. Isshiki, Nucl. Instr. and Meth. B 145 (1998) 80.
- [18] Y. Okazaki et al., Phys. Lett. A 271 (2000) 110.